# DEEP LEARNING TECHNIQUES FOR PREDICTION OF NON-VISUAL LUMINOUS CONTENT OF CELLULAR OFFICES


## Summary

Simulation evaluation of non-image-forming (NIF) effects of daylight in the built environment necessitates using computationally demanding and specialised software. Therefore, this study introduces an alternative approach by exploring the potential of implementing Artificial Neural Networks (ANNs) to predict NIF effects in unilaterally daylit rectangular office spaces. The ANN models were trained on a dataset generated by simulating 349,445 cases of various office geometric configurations, optical material properties, location, sky types, and time of day in a year. The Circadian Stimulus model achieved the best ANN regression model performance with $R^2$ of 0.965, while the melanopic Equivalent Daylight Illuminance model predicted compliance with minimum requirements with 96.7 % accuracy. The results show the practical implications of ANN models for fast prediction of NIF effects in the built environment, significantly reducing the time and effort required for such evaluations and particularly suited for early-stage design phases.


*Keywords: Non-image forming effects, Neural networks, Prediction, Parametric study, Daylight*

## 1. Introduction

Over the past two decades, scientific findings have established that daylight is the primary synchroniser of the circadian rhythms in almost all organisms on Earth. The discovery of Intrinsically Photosensitive Retinal Ganglion Cells (ipRGC) introduced a new dimension to our understanding of light's effect on humans. These cells contain the photopigment melanopsin, which has a maximum sensitivity to light between 460 and 480 nm (Bailes and Lucas, 2013). The impact of light on the circadian system is also substantially influenced by the intensity and temporal characteristics of light stimuli. Evaluating light from a non-image-forming (NIF) perspective is, therefore, much more complex than evaluating the visible effects of light. Unlike the visual effects of daylight, which are usually determined on a horizontal plane at a height of 0.85 m (at the level of desk work), the circadian aspects of daylight are evaluated on a vertical plane at 1.2 m above the ground, which matches the average cornea height of a seated occupant. Furthermore, the received spectral power distribution (SPD) may differ significantly with the orientation of the gaze despite identical positioning in the space (Potočnik and Košir, 2021).

Several metrics have been established in the literature to describe light from the perspective of the circadian system. One key metric is the equivalent α-opic lux, which describes light based on the efficacy curves of each photopigment and follows a methodology comparable to the calculation of photometric lux. Equivalent Melanopic Lux (EML) is commonly used to quantify circadian influence among equivalent α-opic metrics(Lucas et al., 2014). This methodology was also adopted by the International Commission on Illumination – CIE(CIE S 026/E, 2018). The CIE, furthermore, proposed two additional metrics: the melanopic Equivalent Daylight Illuminance (mEDI), which depicts the measured source's equivalent of non-image-forming effect relative to the D65 illuminant, and the Equivalent Melanopic Irradiance (EMI), which represents a melanopically weighted irradiance. A scientific consensus was achieved in 2022 by Brown et al. (2022) that 250 lx (mEDI) during daytime indoors is the recommended target quantity of light for optimal physical and mental health and performance. Rea et al. (2005, 2010), proposed an alternative method for assessing the circadian aspects of light the Circadian Light (CLA). CLA considers the contribution of all photoreceptors involved in NIF light perception. CLA of 1000 represents the effect of 1000 lx of standard CIE illuminant A on the NIF system. Moreover, the CLA method is directly linked to the Circadian Stimulus (CS) metric, where the CS represents the intensity of suppression of nocturnal melatonin. CS of 0.3 means 30 % suppression of nocturnal melatonin and corresponds to 275 CLA. The value of 0.3 CS has been confirmed by several studies (Figueiro and Rea, 2016; Figueiro, 2017; Figueiro et al., 2018) as effective in reducing fatigue and drowsiness


Selection and/or peer review under responsibility of Scientific Committee
10.18086/eurosun.2024.01.10 Available at http://proceedings.ises.org

and improving attention and alertness in human subjects.

To accurately assess the NIF daylight conditions through simulations, software capable of multi-spectral simulations is necessary so that the SPD of light can be calculated at a given point. However, established approaches and tools for visible light simulations, which calculate light in three channels (R, G, B), are inadequate for this task. Currently, LARK (Inanici and LLP, 2015) and ALFA (LLC Sollemma, 2020) are the two most used software tools for simulating NIF effects in buildings. Of these, only ALFA utilises the built-in libRadtran (Emde et al., 2016) solar radiative transfer library to evaluate spectral radiation data of the climate-conditioned sky in determination of indoor SPD. Both tools, however, require significant computation time, suitable hardware, and high user input.

Both daylight and circadian simulations are computationally demanding and time-consuming, making them less appealing to practitioners who face iterative design on a daily basis (Ayoub, 2020). However, in the last decade, we have witnessed the expansion of artificial intelligence (AI), which enables faster acquisition of results based on predictive models offered within the vast field of AI predictive techniques. In the past decade, machine learning and deep learning techniques, such as Artificial Neural Networks (ANN), have been increasingly used in daylighting and lighting applications (Ngarambe et al., 2022). Between 2006 and 2023, over 30 relevant studies on machine learning applications in daylighting have been published (Liu et al., 2023), pointing to a growing interest in the subject. Machine learning has been employed to predict light levels and control various machine-controlled building components such as shades (Xie and Omidfar Sawyer, 2021) or automatic control of luminaires (Park et al., 2019) to ensure the appropriate indoor light levels. Machine learning and deep learning techniques offer an alternative to traditional simulation methods. They can be used to develop models that replace complex simulation tools, particularly in the early design stages. However, these approaches rely on robust databases for training the models. Many machine learning techniques are currently known, and approaches such as support vector machines – (SVM) are most commonly used in the literature for logical control. However, the most commonly used method reported in the literature for predicting the luminous environment is back propagation neural network (BPNN) (Liu et al., 2023), which is a type of ANN. Liu et al. (2023) have identified BPNN as the most efficient method for the regression of light quantity in the built environment. However, these studies addressed only the visual aspects of daylight (Ahmed et al., 2011), artificial illumination (Bellochio et al., 2011) or daylight in combination with building energy performance (Wu et al., 2024). Typically, annual daylight metrics such as Useful Daylight Illuminance (UDI), spatial Daylight Autonomy (sDA), and Annual Sunlight Exposure (ASE) are predicted. For example, Han et al. (2021) have developed an early-stage design framework for BIM, which, based on the data available in the BIM model, can predict the UDI using BPNN techniques. Tests on a single room have shown high accuracy of the model with mean average percentage error (MAPE) under 10 %. Similarly, using BPNN, Lin and Tsay (2021) have predicted the ASE and sDA of different façade designs using the novel concept of pre-processor and intermediary features, which enabled the expansion of the model's application scope. Li et al. recently demonstrated (2024) that absolute values of daylight illuminance can also be predicted using ANN. They used a Generative Adversarial Network to generate daylight predictions, which saved 73 % of the computational time compared to the time required by the simulations with a mean average percentage error of 0.135.

Although significant advancements have been made in applying ML and ANN algorithms for daylight prediction, our literature review revealed that no ML or ANN models currently predict the NIF aspects of daylight. This study aims to address this gap by creating a spectral simulation database and developing ANN models based on that database. In this study, we aim to develop the following models:

- An ANN model for predicting Equivalent Melanopic Illuminance – EML regression model.
- An ANN model for predicting melanopic Equivalent Daylight Illuminance – mEDI regression model.
- An ANN model for predicting Circadian Stimulus – CS regression model.
- Classification ANN models for predicting compliance with EDI or CS requirements – CS and mEDI classification models.

## 2. Methodology

To achieve the research objectives of environment developing predictive models for NIF environment, the

study implemented the following phases (Fig. 1): 1. Simulation model definition; 2. Data generation; 3. Feature selection /engineering; 4. ANN development and evaluation.

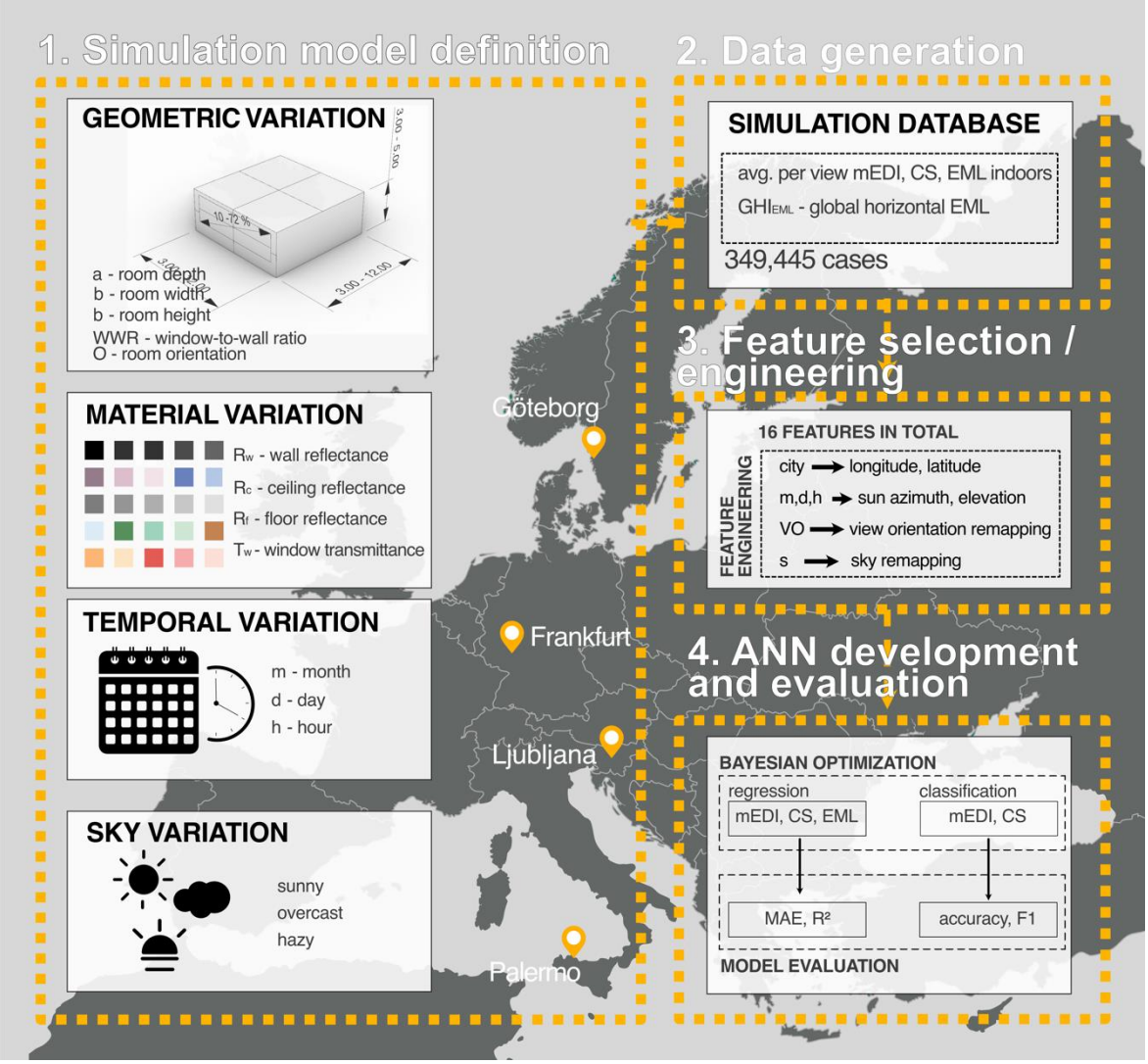


**Fig. 1: Workflow diagram of developed prediction models.**

### 2.1. Simulation Model Definition

To provide a universal model, it was first necessary to determine the appropriate input parameters and their range for the simulation database upon which the ANN models were trained. Simulation models were created upon variation of 15 simulation variables. They can be divided into five main categories (see Tab. 1). The first category includes geometric parameters. The prediction models were limited to rectangular floor plans with unilateral façade openings. Consequently, the geometry of the space can be described by four parameters: depth (a), width (b), and height (h) of the space, as well as Window-to-Wall-Ratio (WWR). The window was fixed at a parapet height of 0.85 m, while cardinal directions of east, south, west and north were considered for its orientation (O). The last geometric parameter was the view orientation (VO) of the considered hypothetical occupant at a corneal height of 1.2 m above the finished floor. The hypothetical occupant positions were placed on a grid with 0.5 x 0.5 m spacing and an offset of 0.25 m from the walls. The grid size depends on the variation of the a and b parameters (see Tab 1). The second category included optical properties of the considered geometric elements. The melanopic reflectivity of walls ($R_{w\text{-}m}$), ceiling ($R_{c\text{-}m}$) and floor ($R_{f\text{-}m}$) were modified. Similarly, the melanopic ($T_{w\text{-}m}$) transmittance of glazing was varied. The third category of temporal parameters included the variation of the month (m), days (d) and hours in a day (h), while only the daylit part was considered. The last category included climate variables of location and sky type variation. Sky was modelled as sunny, hazy, and overcast, and the locations considered were Göteborg (57.71° N, 11.97° E), Frankfurt (50.11° N, 8.68° E), Ljubljana (46.05° N, 14.51° E), and Palermo (38.12° N, 13.36° E).

**Tab. 1: Simulation model variables.**

| Group | Parameter | Min | Max | Step |
|---|---|---|---|---|
| Geometric parameters | Depth - a [m] | 3 | 12 | 2.25 |
| | Width - b [m] | 3 | 12 | 2.25 |
| | Height - c [m] | 3 | 12 | 2.25 |
| | WWR [%] | 10 | 72 | varies |
| | View orientation - VO [°] | 0 | 270 | 90 |
| | Room orientation - O [°] | 0 | 270 | 90 |
| Temporal parameters | Month - m | 1 | 11 | 2 |
| | Day – d | 1 | 30 | 15 |
| | Hours in a day - h [h] | 7 | 21 | varies |
| Optical parameters | $R_{w\text{-}m}$ [%] | 10 | 100 | varies |
| | $R_{f\text{-}m}$ [%] | 10 | 100 | varies |
| | $R_{c\text{-}m}$ [%] | 10 | 100 | varies |
| | $T_{g\text{-}m}$ [%] | 10 | 100 | varies |
| **Group** | **Parameter** | **Categorical input** | | |
| Climate parameters | Location | Frankfurt, Ljubljana, Göteborg, Palermo | | |
| | Sky type | clear sky, hazy sky, overcast sky | | |

### *2.2. Data Generation*

All potential simulation parameter variations would result in over 1 x $10^9$ cases. Therefore, a random selection script was run on all possible parameter permutations to select 349,445 cases to be modelled, simulated and included in the simulation database. The required geometric models were created using a custom script in Grasshopper and baked into layers in Rhinoceros accordingly. The geometry from Rhinoceros was then fed to the multispectral simulations, which were performed using the multispectral raytracing software plugin for Rhinoceros ALFA (LLC Sollemma, 2020). ALFA is a well-established and reliable simulation tool for multispectral simulations of daylight (Diakite-Kortlever and Knoop, 2021; Potočnik and Košir, 2022). The mentioned software uses libradtran (Emde et al., 2016), a radiative transfer calculation software package for calculating the spectral sky according to the geographic location. It can calculate four different sky types: clear, hazy, overcast and heavy rain cloudy from the atmospheric profile for midlatitude locations. Since ALFA does not offer a batch function to simulate numerous study cases, a Python script with PyAutoGUI for graphical user interface automation was used to automate simulations by controlling the computer mouse pointer and keyboard input. The automation script and the simulation models were deployed to 25 individual computers connected to a common network, which simultaneously calculated the simulations and built a database of all simulation outcomes. The spectral daylight calculations were performed at the following settings for each case: ambient bounces – (ab) 8, limit weight (lw) 0.001 at 200 passes for each simulation. Default ALFA results include data such as SPD, EML, and lx. For this study's ANN regression models, the photopic illuminance data was discarded, and SPD was used to calculate the mEDI and CS values. Afterwards, average values per case variation and occupant view orientation were calculated for each of the selected metrics. In the end, for the classification models, the average values mentioned before were evaluated according to the NIF requirement criteria for mEDI of $\geq$ 250 lx and $\geq$ 0.3 CS and output into the binary output of 0, meaning it does not meet the criteria, and 1, meaning the value meets the criteria.

### *2.3. Feature engineering and selection*

In total, 14 properties (see Tab. 1) defined the simulation iterations performed to obtain the simulation data; however, for the ANN training, 16 variables were selected/derived (Fig. 2). All the input variables were coded as continuous. Sky was transformed from a categorical to a continuous variable where clear = 1, hazy = 0.5

and overcast = 0. Room orientation with window facing north equalled to 0°, the east oriented room was coded to 90° etc., in a clockwise direction. View orientation was coded so that the 0° view was always facing the window with other views coded in 90° increments clockwise accordingly. The location property was coded into longitude and latitude. The input combination of longitude, latitude, hour, day and month was used to calculate sun azimuth and elevation. Global horizontal EML ($GH_{EML}$) data were gathered directly from the database. Other variables were input directly from the simulation model development. As can be seen in the correlation matrix in Fig. 2, no multicollinearity was present in the predictors. A stronger correlation of 0.81 between sun altitude and $GH_{EML}$ was present, but the $GH_{EML}$ was not dropped since it directly affects indoor illuminance – higher/lower outdoor illuminances translate directly to higher/lower indoor illuminances.

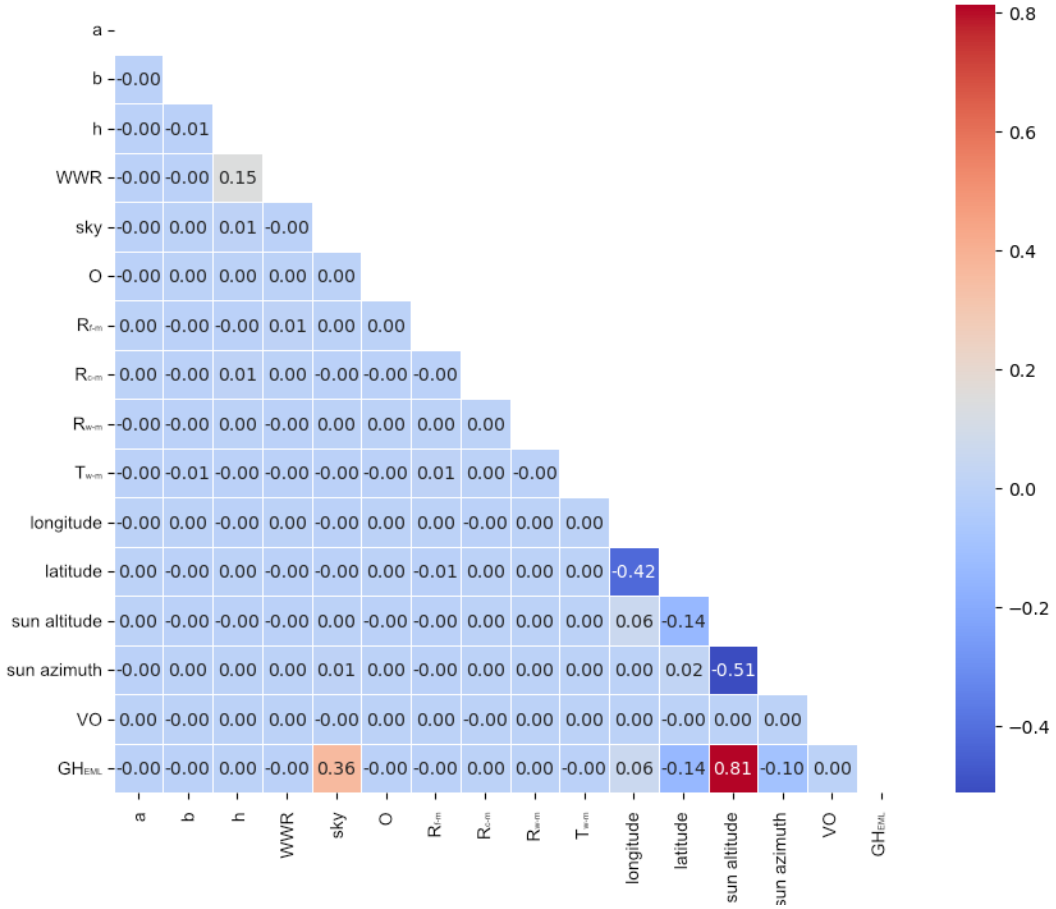


**Fig. 2: Correlation matrix of input variables for ANN models.**

### *2.4. Neural Network Model Development*

Neural networks are computational models inspired by the human brain's structure and functioning, designed to recognise patterns, learn from data and make predictions. They consist of nodes – neurons that receive input data – signal, process it, and produce an output. The nodes are usually connected using connections-weights, which are adjusted during learning and influence the signal's strength and direction to the next neuron. The connections between neurons are transformed using non-linear transformations. These functions introduce non-linearity into the network to learn complex patterns. Two different non-linear transformation functions, rectified linear unit function (ReLU) and hyperbolic tangent function (tanh), were explored for the regression of ANN models, and three different functions, ReLU, tanh and sigmoid, were explored for the classification ANN models.

The neurons of an ANN model are organised into layers. First is the input layer, which matches the number of input variables used for the predictive model. For this study, each developed model had 16 input variables and one output layer. In between, an optimal number of hidden layers (hl) was determined for each developed model simultaneously with the number of neurons per hidden layer (n). The data input to the model follows

the principle of forward propagation, meaning that the input data is fed into the network, and the computations proceed layer by layer from input to output, producing a final prediction. To minimise the difference between the network's prediction and actual target values, a backpropagation learning algorithm was used, where the principle of gradient descent is used to propagate the error backwards through the network to minimise the loss function (i.e. mean average error – MAE for regression tasks and binary cross-entropy for the classification tasks) using an optimisation algorithm that updates the model parameters. Two different optimisation algorithms were explored in the development of ANNs for this study Root Mean Square Propagation (RMSProp) and Adaptive Moment Estimation (ADAM), which are controlled by the learning rate (lr). The learning rate determines the step size at each iteration while moving towards the minimum of the loss function. Two general types of ANN models for predicting non-visual luminous environments were developed for this study. The first model type are regression ANN models, developed for the prediction of EML, CS and mEDI, expressing the absolute NIF luminous content. The second type of ANN model was the classification model, which predicted whether the average CS and mEDI of the space passed their respective requirements.

ANN's ability to learn depends on the structure and other hyperparameters. Furthermore, the optimal hyperparameters vary from case to case. There are three most commonly used methods to determine the optimal structure of an ANN: random search (James Bergstra and Yoshua Bengio, 2012), grid search (Pontes et al., 2016) or hyperparameter optimisation using Bayesian optimisation (Snoek et al., 2012). The first two methods are brute force principles, which demand the calculation of a large pool of different parameter combinations to find the optimal model performance. In this study, a substantial amount of training data (349 445) was collected to build the ANN models. Consequently, a large average calculation time was expected to be required to train a single ANN model. Therefore, the Bayesian optimisation of hyperparameters was used to find the optimal models. Bayesian optimisation uses a surrogate model, a Gaussian Process, to approximate the objective function of hyperparameters. It utilises an acquisition function to decide which hyperparameters to evaluate next, balancing exploration and exploitation. This process iterates until the optimal hyperparameters are found or a stopping criterion is met, making it a highly efficient method for hyperparameter tuning in ANNs (Snoek et al., 2012). In the search for the optimal models, we have identified six hyperparameters, which would be optimised using Bayesian optimisation. As shown in Tab. 2, the chosen hyperparameters to be optimised were: number of hidden layers (hl), number of neurons per layer (n), batch size (bs), optimiser (opt), activation function (a_f) and learning rate (lr). The Bayesian optimisation was applied to TensorFlow models using the Bayesian optimisation API (Nogueira, 2014).

**Tab. 2: Results of the performed ANN regression models.**

| Hyperparameter name | Optimization pool |
|---|---|
| hl | 1 – 6 hidden layers |
| n | 16 – 128 neurons |
| bs | 32 – 256 samples |
| opt | ADAM, RMSProp, |
| a_f | RELU, tanh , sigmoid |
| l_r | 0.00001-0.001 |

Data used for the training of models was split into training, validation and test datasets in a ratio of 70/20/10 %. All models were configured to train for up to 300 epochs, with the training process governed by an early-stopping algorithm. The patience parameter was set to 10 epochs, meaning the algorithm would wait for 10 epochs for any improvement in the model's validation metric. The training would halt if no improvement was observed within these ten epochs. This approach effectively prevented the potential overfitting of the models. The algorithm was set to select the best training weights along this process.

### *2.5. Model evaluation*

Both regression and classification models were evaluated using commonly used evaluation metrics in machine learning. Regression models were evaluated using mean average error (MAE) presented in eq. 1 and coefficient of determination ($R^2$).

$$MAE = \frac{1}{n}\sum_{i=1}^{n}|y_i - \hat{y}_i| \qquad \text{(eq. 1)}$$

Classification models were evaluated using Accuracy rating (eq. 2), which is the ratio of correctly predicted instances (TP – true positive and TN – true negative values) to the total of instances (including FP – false positive and FN – false negative values), the ratio of 1 presents a perfect score. Additionally, models were tested using the F1 score (eq. 5), which, in addition to Precision rate (accuracy of positive predictions – eq. 4), evaluates recall rate (false positive occurrence – eq. 3), a value of 1 presents perfect F1 score.

$$Accuracy = \frac{TP+TN}{TP+TN+FP+FN} \qquad \text{(eq. 2)}$$

$$Recall = \frac{TP}{TP+FN} \qquad \text{(eq. 3)}$$

$$Precision = \frac{TP}{TP+FP} \qquad \text{(eq. 4)}$$

$$F1 = 2 \times \frac{Precision \times Recall}{Precision+Recall} \qquad \text{(eq. 5)}$$

## 3. Results

### 3.1. Dataset results

The dataset contains calculated values for the NIF environment simulations obtained from the ALFA simulations. Fig. 3, presents the simulation data distribution used to train the model. Most EML values ranged from 240 EML (Q1) to 1869 EML (Q3), with a median value of 707 EML and an average of 1788 lx. Similarly, the mEDI values ranged from 217 lx (Q1) to 1693 lx (Q3), with a median value of 640 lx and an average of 1620 lx. The CS values are defined on a logarithmic scale between 0 and 0.7. The database yielded a median value of 0.48 CS, with most data falling between 0.29 CS (Q1) and 0.61 CS (Q2) and an average of 0.44 CS.

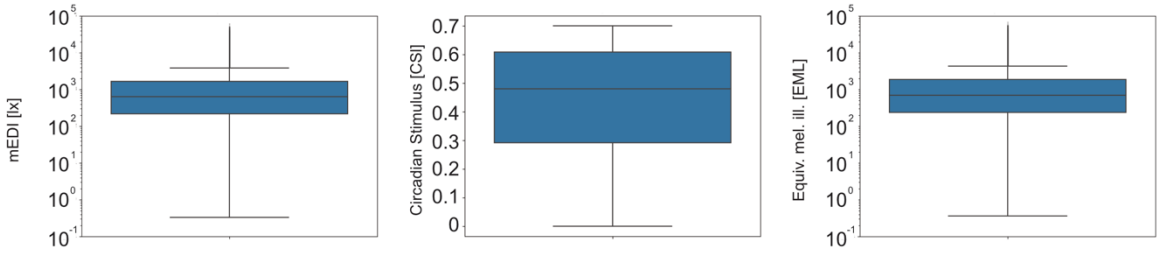


**Fig. 3: Data gathered for the EML, CS and mEDI prediction models.**

### 3.2. ANN regression model results

Based on the dataset's calculated NIF values presented in section 3.1, three ANN regression models were developed using the Bayesian optimisation process. The optimal hyperparameters and resulting prediction accuracy are shown in Tab. 3. The Bayesian optimisation has effectively tuned the models, with the CS regression model emerging as the most effective in explaining variance ($R^2$). The CS model reached the best performance in terms of $R^2$ score (0.965), indicating it explains 96.5 % of the variance, which can be considered an excellent result. In addition, it is also worth mentioning that the CS model required the least complex structure among presented models, namely four hidden layers with 96 neurons each were required by the optimal CS regression model. In contrast, both EML and mEDI required five hidden layers with 120 and 123 neurons for EML and mEDI regression models respectively. Despite having a more complex structure, the regression models performed excellently with 91.1 % and 91.2 % of variance explained for the EML and EDI models, respectively.

**Tab. 3: Results of the performed ANN regression models.**

**ANN regression models**

| M | #f | h-l | n | b_s | a_f | opt | lr | $MAE_{train}$ | $MAE_{val}$ | $MAE_{test}$ | $R^2$ |
|---|---|---|---|---|---|---|---|---|---|---|---|

| | | | | | | | | | | | |
|---|---|---|---|---|---|---|---|---|---|---|---|
| EML | 14 | 5 | 120 | 46 | RELU | RMSProp | 0.001 | 186.4 | 188.9 | 181.1 | 0.911 |
| CS | 14 | 4 | 96 | 123 | RELU | ADAM | 0.001 | 0.0117 | 0.0126 | 0.0135 | 0.965 |
| EDI | 14 | 5 | 123 | 49 | RELU | ADAM | 0.0009 | 163.32 | 168.13 | 165.5 | 0.912 |

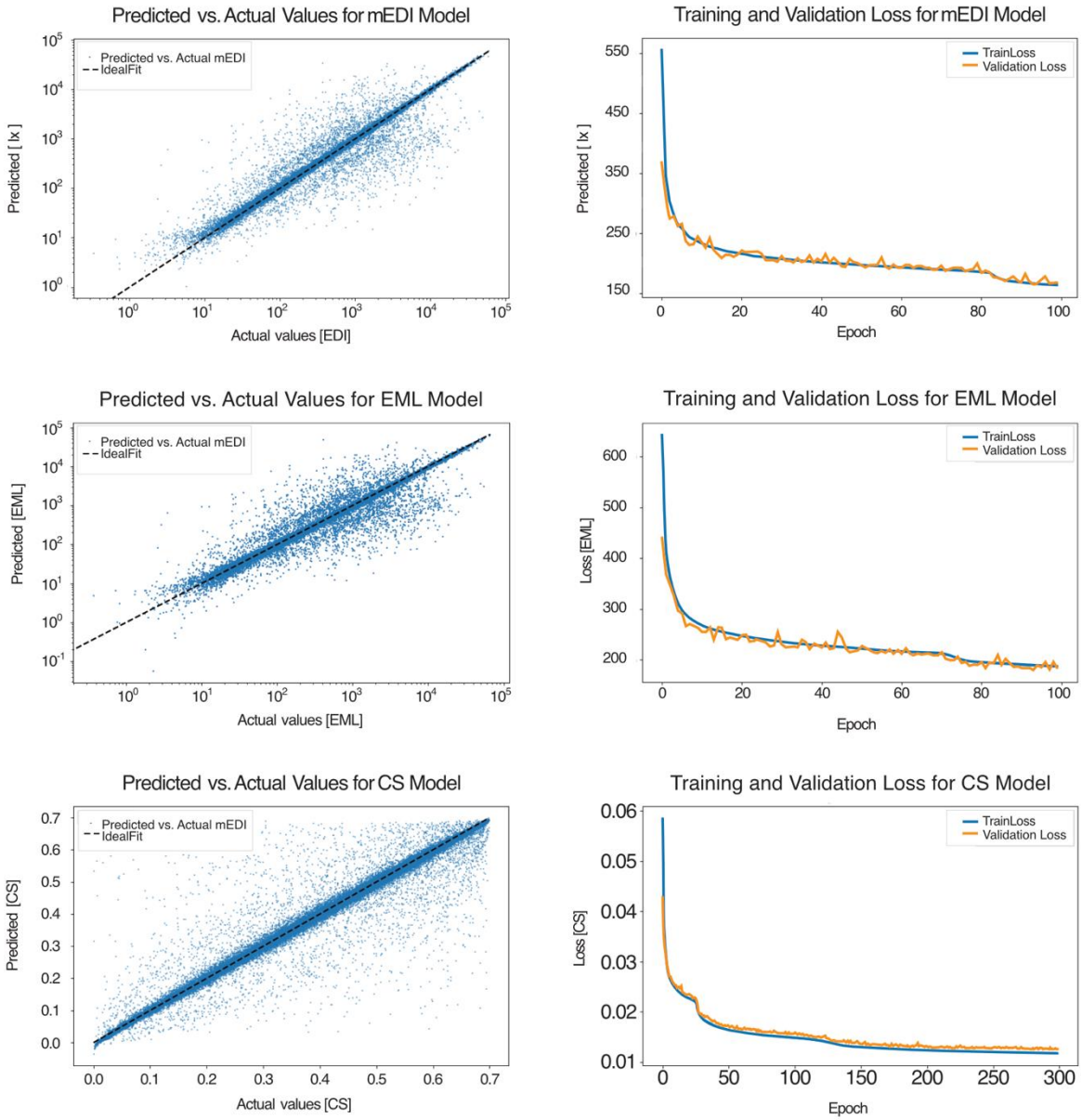


**Fig. 4: Performance and training process of regression ANN regression models.**

Each regression model shows consistent performance and good generalisation ability, which is expressed by slight differences in performance between training ($MAE_{train}$), validation ($MAE_{val}$), and test ($MAE_{test}$) datasets (Tab. 3). The small difference in $MAE_{test}$ is particularly significant, as it describes the model's performance on unseen data. If the model were overfit, the $MAE_{test}$ would result in considerably higher errors. As shown in Fig. 4. all models learned well, with good convergence and stable training performance. No major deflection of validation loss (orange lines in Fig. 4) can be detected for either of the models, which would indicate overfitting. Both mEDI and EML models stopped at the 98$^{th}$ epoch, while the CS model's training was stopped at the 287$^{th}$ epoch. Predicted vs. actual values plots of models in Fig. 4 show the best performance for the mEDI regression model in the range between $10^1$ and $10^2$ mel lx and approximately $10^4$ and $10^5$ mel lx. A similar is true for the EML regression model. Meanwhile, the CS model shows almost consistent performance throughout the entire range, with slightly higher inaccuracy between 0.6 and 0.7 CS.

### 3.3. ANN classification model results

The optimal model architecture and hyperparameter values for the ANN classification models performed in this study are shown in Tab. 4. As seen from the table, these data introduced much less complexity than the data for regression models (see Tab. 3) and required considerably simpler model architectures. CS compliance classification prediction model required two hidden layers with 32 neurons using a sigmoid activation function with a 0.0002 learning rate and a batch size of 32 samples. The model performed excellently, as expressed by the 96.7 % accuracy on the training dataset ($acc_{train}$). Tests on validation data ($acc_{val}$) and test data ($acc_{test}$) also expressed excellent performances with a difference in performance on validation and test dataset compared to the training dataset with only 0.3 percentage points (pp) for each respective dataset. When testing the model's performance by evaluating false positive and false negative predictions, the F1 score showed that the model performed at an even higher precision rating of 97 % on the test dataset. mEDI compliance classification model's structure, similar to the CS model, required lower complexity than the regression models to achive optimal performance. The optimal architecture of the model was found at six hidden layers with 16 neurons per layer at a learning rate of 0.0006 and 123 batch sample size. Similarly, to the CS classification model, mEDI used a sigmoid activation function and ADAM optimiser. The model resulted in even higher accuracy on the train data set of 97 % with $acc_{val}$ and $acc_{test}$ with comparable accuracy (Tab. 4) and the difference to the $acc_{train}$ performance of only 0.1 pp and 0.3 pp, respectively. The F1 score of 97.7 % is almost the same as for the CS classification model, indicating robust performance.

**Tab. 4: Results of the performed ANN classification models.**

| Classification models | | | | | | | | | | | |
|---|---|---|---|---|---|---|---|---|---|---|---|
| **M** | **#f** | **hl** | **n** | **b_s** | **a_f** | **opt** | **lr** | **$acc_{train}$** | **$acc_{val}$** | **$acc_{test}$** | **F1** |
| CS | 14 | 2 | 32 | 32 | sigmoid | ADAM | 0.0002 | 0.967 | 0.964 | 0.964 | 0.970 |
| mEDI | 14 | 6 | 16 | 123 | sigmoid | ADAM | 0.0006 | 0.970 | 0.969 | 0.967 | 0.977 |

Fig.5 shows the training process of the presented CS and mEDI classification prediction models. Both models show good convergence with no possible overfitting of the models, and no notable deflection between the accuracy and validation loss was detected with the models. CS model's early stopping algorithm stopped the learning at the 53$^{rd}$ epoch, while mEDI's early stopping algorithm halted the training at the 74$^{th}$ epoch, thus prohibiting possible overfitting of the model. As mentioned before, minute differences in $acc_{train}$, $acc_{val}$ and $acc_{test}$ express that overfitting is not present. Therefore, we can say the model generalises well.

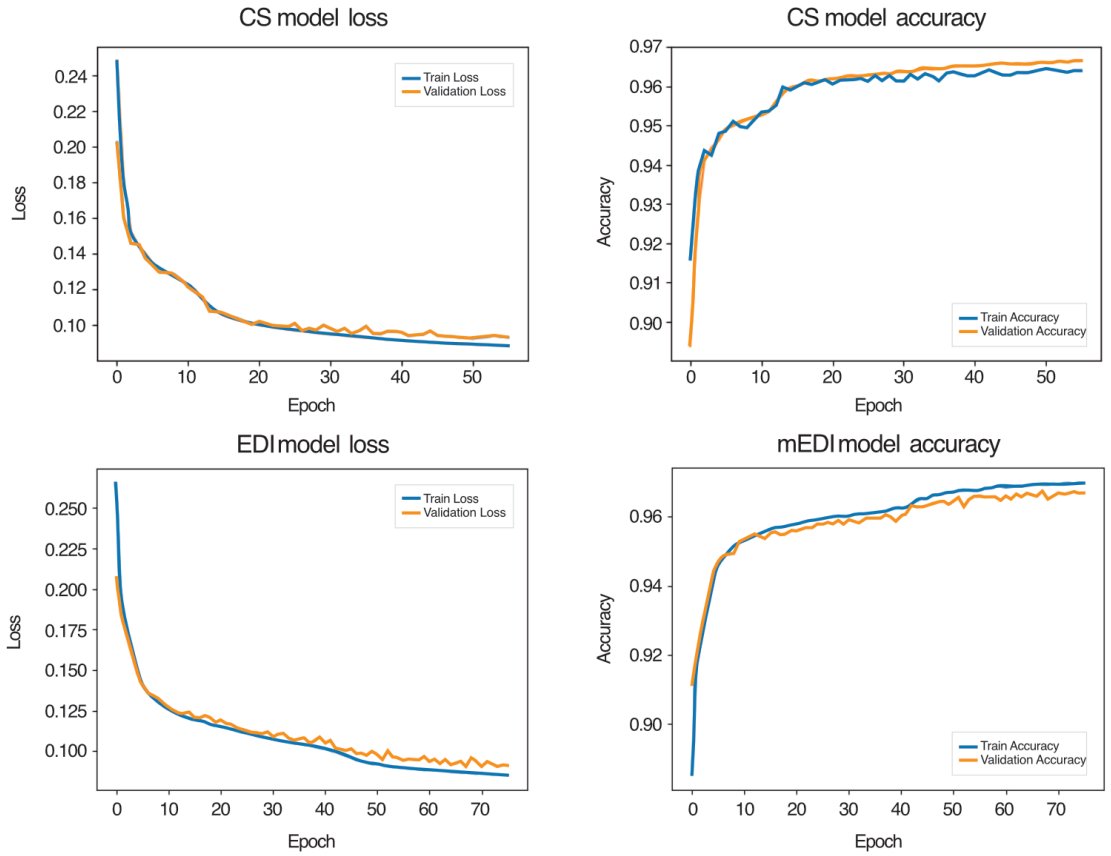


**Fig. 5: Performance of classification ANN models.**

## 4. Discussion and Conclusion

The presented study introduced a novel framework for predicting the NIF indoor potential of unilaterally lit spaces. We have successfully developed an NIF simulation database, which served as a training basis for the development of predictive Artificial Neural Networks, using backpropagation algorithms. The Bayesian Optimisation methodology of hyperparameter optimisation was successfully applied to the framework, where model hyperparameters were optimised to develop accurate prediction models of the NIF environment. The best-performing model among regression models was the Circadian Stimulus (CS) model, whose predictions were able to explain 96.5 % of the variance. The Equivalent Melanopic Illuminance (EML) and melanopic Equivalent Daylight Illuminance (mEDI) models also performed well, with over 91 % of explained variance in the test predictions. Additionally, two classification models were trained using the ANN methodology. The same Bayesian Optimisation algorithm was applied to the models to find the optimal architecture of the models. As a result, models could discern the compliance of the average CS or mEDI requirements for healthy luminous environments. Both model's accuracy was exerted at over 97 %.

The results have shown that the NIF properties of indoor environments can be predicted using the principles of deep learning, specifically Artificial Neural Networks. Results from the trained models can be used by the practitioners for early-stage building design checking in regard to the designed space NIF luminous aspects. They can also be used as an informative tool by property managers or occupants to assess the NIF potential of their properties without the need for complex and lengthy simulations. Such models, due to their fast performance (1 input into ANN predictive model is calculated in 850 µs), could potentially, in future studies, be used on annual weather data, which would enable the prediction of yearly NIF potentials of the validated unilaterally lit spaces.

Nevertheless, it is essential to recognise that the study's findings are confined to average room values and do not account for spatial variations in the space. Moreover, the current model is restricted to rooms daylit through a single window on one façade and rectangular room geometries. Currently, the models were developed based

on data from just four locations. For more accurate predictions at other latitudes, it would be necessary to include data from additional locations. Future efforts should aim to develop models capable of predicting NIF daylight potential based on specific sensor positions within a room, enabling the evaluation of the spatial distribution of daylight within the considered space. In addition, further research is needed to assess prediction accuracy in spaces illuminated from multiple directions.

## 5. Acknowledgments

The presented research resulted from a project, *Calculation of Yearly Circadian Potential in Buildings Using Deep Learning Techniques—YCPdeep* (project No. J2 – 3036), funded by the Slovenian Research and Innovation Agency (project No. J2 – 3036). The authors also acknowledge the financial support from the Slovenian Research and Innovation Agency research core funding No. P2 – 0158.

## 6. References

Ahmed, A., Otreba, M., Korres, N.E., Elhadi, H., Menzel, K., 2011. Assessing the performance of naturally day-lit buildings using data mining. Advanced Engineering Informatics 25, 364–379. https://doi.org/10.1016/j.aei.2010.09.002

Ayoub, M., 2020. A review on machine learning algorithms to predict daylighting inside buildings. Solar Energy 202, 249–275. https://doi.org/10.1016/J.SOLENER.2020.03.104

Bailes, H.J., Lucas, R.J., 2013. Human melanopsin forms a pigment maximally sensitive to blue light (λmax ≈ 479 nm) supporting activation of Gq/11 and Gi/o signalling cascades. Proc. R. Soc. B 280, 20122987. https://doi.org/10.1098/rspb.2012.2987

Bellochio, F., Ferrari, S., Lazzaroni, M., Cristaldi, L., Rossi, M., Poli, T., Paolini, R., 2011. Illuminance prediction through SVM regression, in: IEEE Workshop on Environmental Energy and Structural Monitoring Systems. Milan, Italy, pp. 1–5. https://doi.org/10.1109/EESMS.2011.6067051

Brown, T.M., Brainard, G.C., Cajochen, C., Czeisler, C.A., Hanifin, J.P., Lockley, S.W., Lucas, R.J., Münch, M., OHagan, J.B., Peirson, S.N., Price, L.L.A., Roenneberg, T., Schlangen, L.J.M., Skene, D.J., Spitschan, M., Vetter, C., Zee, P.C., Wright, K.P., 2022. Recommendations for daytime, evening, and nighttime indoor light exposure to best support physiology, sleep, and wakefulness in healthy adults. PLoS Biol 20, e3001571. https://doi.org/10.1371/JOURNAL.PBIO.3001571

CIE S 026/E:2018, 2018. CIE System for Metrology of Optical Radiation for ipRGC-Influenced Responses to Light CIE S 026/E:2018.

Diakite-Kortlever, A.K., Knoop, M., 2021. Forecast accuracy of existing luminance-related spectral sky models and their practical implications for the assessment of the non-image-forming effectiveness of daylight: Lighting Research & Technology 53, 657–676. https://doi.org/10.1177/1477153520982265

Emde, C., Buras-Schnell, R., Kylling, A., Mayer, B., Gasteiger, J., Hamann, U., Kylling, J., Richter, B., Pause, C., Dowling, T., Bugliaro, L., 2016. The libRadtran software package for radiative transfer calculations (version 2.0.1). Geosci Model Dev 9, 1647–1672. https://doi.org/10.5194/gmd-9-1647-2016

Figueiro, M., Rea, M., 2016. Office lighting and personal light exposures in two seasons: Impact on sleep and mood. Lighting Research & Technology 48, 352–364. https://doi.org/10.1177/1477153514564098

Figueiro, M.G., 2017. Disruption of Circadian Rhythms by Light During Day and Night. Curr Sleep Med Rep 3, 76–84. https://doi.org/10.1007/s40675-017-0069-0

Figueiro, M.G., Nagare, R., Price, L.L.A., 2018. Non-visual effects of light: How to use light to promote circadian entrainment and elicit alertness. Lighting Research & Technology 50, 38–62. https://doi.org/10.1177/1477153517721598

Han, Y., Shen, L., Sun, C., 2021. Developing a parametric morphable annual daylight prediction model with improved generalization capability for the early stages of office building design. Build Environ 200, 107932. https://doi.org/10.1016/J.BUILDENV.2021.107932

Inanici, M., LLP, Z.A., 2015. Lark Spectral Lighting [WWW Document]. URL http://faculty.washington.edu/inanici/Lark/Lark_home_page.html (accessed 10.30.20).

James Bergstra, Yoshua Bengio, 2012. Random Search for Hyper-Parameter Optimization. Journal of

Machine Learning Research 13, 281–305.

Li, X., Yuan, Y., Liu, G., Han, Z., Stouffs, R., 2024. A predictive model for daylight performance based on multimodal generative adversarial networks at the early design stage. Energy Build 305, 113876. https://doi.org/10.1016/J.ENBUILD.2023.113876

Lin, C.H., Tsay, Y.S., 2021. A metamodel based on intermediary features for daylight performance prediction of façade design. Build Environ 206, 108371. https://doi.org/10.1016/J.BUILDENV.2021.108371

Liu, Q., Chen, Y., Liu, Y., Lei, Y., Wang, Y., Hu, P., 2023. A review and guide on selecting and optimizing machine learning algorithms for daylight prediction. Build Environ 244, 110822. https://doi.org/10.1016/J.BUILDENV.2023.110822

LLC Sollemma, 2020. ALFA - Adaptive Lighting for Alertness [WWW Document]. URL https://www.solemma.com/Alfa.html (accessed 10.30.20).

Lucas, R.J., Peirson, S.N., Berson, D.M., Brown, T.M., Cooper, H.M., Czeisler, C.A., Figueiro, M.G., Gamlin, P.D., Lockley, S.W., O'Hagan, J.B., Price, L.L.A., Provencio, I., Skene, D.J., Brainard, G.C., 2014. Measuring and using light in the melanopsin age. Trends Neurosci 37, 1–9. https://doi.org/10.1016/j.tins.2013.10.004

Ngarambe, J., Adilkhanova, I., Uwiragiye, B., Yun, G.Y., 2022. A review on the current usage of machine learning tools for daylighting design and control. Build Environ 223, 109507. https://doi.org/10.1016/J.BUILDENV.2022.109507

Nogueira, F.M.F., 2014. BayesianOptimization.

Park, J.Y., Dougherty, T., Fritz, H., Nagy, Z., 2019. LightLearn: An adaptive and occupant centered controller for lighting based on reinforcement learning. Build Environ 147, 397–414. https://doi.org/10.1016/j.buildenv.2018.10.028

Pontes, F.J., Amorim, G.F., Balestrassi, P.P., Paiva, A.P., Ferreira, J.R., 2016. Design of experiments and focused grid search for neural network parameter optimization. Neurocomputing 186, 22–34. https://doi.org/10.1016/J.NEUCOM.2015.12.061

Potočnik, J., Košir, M., 2022. ASSESSMENT OF MULTISPECTRAL SIMULATION TOOLS FOR THE EVALUATION OF THE CIRCADIAN LUMINOUS ENVIRONMENT. Gradbeni vestnik 111–125.

Potočnik, J., Košir, M., 2021. Influence of geometrical and optical building parameters on the circadian daylighting of an office. Journal of Building Engineering 42, 102402. https://doi.org/10.1016/j.jobe.2021.102402

Rea, M.S., Figueiro, M.G., Bierman, A., Bullough, J.D., 2010. Circadian light. J Circadian Rhythms 8. https://doi.org/10.1186/1740-3391-8-2/METRICS/

Rea, M.S., Figueiro, M.G., Bullough, J.D., Bierman, A., 2005. A model of phototransduction by the human circadian system. Brain Res Rev 50, 213–228. https://doi.org/10.1016/j.brainresrev.2005.07.002

Snoek, J., Larochelle, H., Adams, R.P., 2012. Practical Bayesian Optimization of Machine Learning Algorithms. Adv Neural Inf Process Syst 25.

Wu, C., Pan, H., Luo, Z., Liu, C., Huang, H., 2024. Multi-objective optimization of residential building energy consumption, daylighting, and thermal comfort based on BO-XGBoost-NSGA-II. Build Environ 254, 111386. https://doi.org/10.1016/J.BUILDENV.2024.111386

Xie, J., Omidfar Sawyer, A., 2021. A simplified open-loop control strategy for integrated shading and lighting systems using machine learning. https://doi.org/10.26868/25222708.2021.30629